doi:10.1093/brain/awr008 Brain 2011: 134; 704–720 | 704

BRAIN
A JOURNAL OF NEUROLOGY

Inhibition of lymphocyte trafficking shields the brain against deleterious neuroinflammation after stroke

Arthur Liesz,[1] Wei Zhou,[1] Éva Mracskó,[1] Simone Karcher,[1] Henrike Bauer,[2] Sönke Schwarting,[1] Li Sun,[1] Dunja Bruder,[3] Sabine Stegemann,[3] Adelheid Cerwenka,[4] Clemens Sommer,[2] Alexander H. Dalpke[5] and Roland Veltkamp[1]

1 Department of Neurology, University Heidelberg, Im Neuenheimer Feld 400, 69120 Heidelberg, Germany
2 Department of Neuropathology, University Medical Centre of the Johannes Gutenberg University Mainz, Langenbeckstrasse 1, 55131 Mainz, Germany
3 Division of Immunregulation, Helmholtz Centre for Infection Research, Inhoffenstraße 7, 38124 Braunschweig, Germany
4 Division of Innate Immunity, German Cancer Research Centre, Im Neuenheimer Feld 280, 69120 Heidelberg, Germany
5 Department of Infectious Diseases, Medical Microbiology and Hygiene, University Heidelberg, Im Neuenheimer Feld 324, 69120 Heidelberg, Germany

Correspondence to: Roland Veltkamp, MD,
Department of Neurology,
University Heidelberg,
Im Neuenheimer Feld 400,
69120 Heidelberg,
Germany
E-mail: roland.veltkamp@med.uni-heidelberg.de

T lymphocytes are increasingly recognized as key modulators of detrimental inflammatory cascades in acute ischaemic stroke, but the potential of T cell-targeted therapy in brain ischaemia is largely unexplored. Here, we characterize the effect of inhibiting leukocyte very late antigen-4 and endothelial vascular cell adhesion molecule-1-mediated brain invasion—currently the most effective strategy in primary neuroinflammatory brain disease in murine ischaemic stroke models. Very late antigen-4 blockade by monoclonal antibodies improved outcome in models of moderate stroke lesions by inhibiting cerebral leukocyte invasion and neurotoxic cytokine production without increasing the susceptibility to bacterial infections. Gene silencing of the endothelial very late antigen-4 counterpart vascular cell adhesion molecule-1 by *in vivo* small interfering RNA injection resulted in an equally potent reduction of infarct volume and post-ischaemic neuroinflammation. Furthermore, very late antigen-4-inhibition effectively reduced the post-ischaemic vascular cell adhesion molecule-1 upregulation, suggesting an additional cross-signalling between invading leukocytes and the cerebral endothelium. Dissecting the specific impact of leukocyte subpopulations showed that invading T cells, via their humoral secretion (interferon-γ) and immediate cytotoxic mechanisms (perforin), were the principal pathways for delayed post-ischaemic tissue injury. Thus, targeting T lymphocyte-migration represents a promising therapeutic approach for ischaemic stroke.

Keywords: brain ischaemia; T cell; VLA-4; VCAM-1; inflammation

Abbreviations: MCAO = middle cerebral artery occlusion; VCAM-1 = vascular cell adhesion molecule-1; VLA-4 = very late antigen-4

Received August 10, 2010. Revised November 29, 2010. Accepted December 15, 2010

Introduction

Ischaemic stroke is a major cause of death and disability worldwide. Because thrombolysis, the only approved therapy for acute stroke at present, reaches only 5–10% of patients, therapeutic alternatives are being sought (Donnan *et al*., 2008). Among many detrimental cascades (Lo *et al*., 2003), inflammatory mechanisms have come into the focus of current research because they contribute substantially to secondary brain damage (Dirnagl, 2004; Wang *et al*., 2006; Hurn *et al*., 2007; Liesz *et al*., 2009*b*). Moreover, their prolonged kinetics make them amenable to therapeutic intervention (Barone and Feuerstein, 1999; Dirnagl *et al*., 1999; Gelderblom *et al*., 2009). Recent experimental studies suggest a pivotal role of T cells in post-ischaemic inflammation of various organs including the brain (Zwacka *et al*., 1997; del Zoppo *et al*., 2001; Frangogiannis *et al*., 2002; Gee *et al*., 2007; Liesz *et al*., 2009*b*; Lo, 2009). However, the potential of T cell-targeted therapy in brain ischaemia is largely unexplored to date.

The presence and activity of systemic immune cells in the healthy brain is restricted and tightly regulated by the intact blood–brain barrier (Engelhardt and Sorokin, 2009). The adhesion of leukocytes to the activated endothelium and subsequent brain invasion after cerebral ischaemia represent critical steps in inducing collateral inflammatory damage. Cerebral invasion of lymphocytes crucially depends on the interaction of the leukocyte very late antigen-4 (VLA-4) with vascular cell adhesion molecule-1 (VCAM-1) on endothelial cells (Baron *et al*., 1993; Engelhardt *et al*., 1998; Laschinger and Engelhardt, 2000; Vajkoczy *et al*., 2001; Engelhardt and Sorokin, 2009). VLA-4 (integrin alpha4-beta1) is an integrin heterodimer consisting of an alpha chain (integrin $\alpha 4$ = CD49d) and a beta chain (CD29) Correspondingly, natalizumab, an antibody blocking $\alpha 4$-integrin-mediated invasion of lymphocytes into the CNS, currently represents the most effective therapy for relapsing-remitting multiple sclerosis (Yednock *et al*., 1992; Rice *et al*., 2005; Steinman, 2005; Polman *et al*., 2006). In contrast, the impact of this potent approach has barely been investigated in stroke.

Herein, we comprehensively examine the profound effect of inhibition of the VLA-4–VCAM-1 axis on secondary tissue injury after experimental brain ischaemia, and uncover reduced T lymphocyte-mediated cytotoxicity as the key underlying mechanism of action.

Materials and methods

Animals

The study was conducted in accordance with national guidelines for the use of experimental animals and the protocols were approved by the governmental committees (Regierungspraesidium Karlsruhe, Germany). We used age-matched, male mice (C57BL/6J, 10–12 weeks, 23–25 g body weight, Charles River Laboratories) unless stated otherwise. For transfer experiments, lymphocyte-deficient *Rag2*$^{-/-}$ mice were used as recipients. Perforin knockout mice *Prf1*$^{-/-}$ were purchased from The Jackson Laboratory. The genetic background of *Rag2*$^{-/-}$ and *Prf1*$^{-/-}$ animals were fully comparable with that of the respectively used wild-type control animals (backcrossed for at least 10 generations).

Animal experiments

We injected 300 μg of CD49d-specific monoclonal antibody (clone R1-2, free of azide and preservatives) intraperitoneally (i.p.) 24 h before or 3 h after ischaemia-induction, control animals received rat IgG2b isotype control monoclonal antibody. Antibodies were commercially purchased from eBioscience. See Supplementary Materials for detailed descriptions of the ischaemia models.

Assessment of infarct volume

The mice were deeply anaesthetized and perfused transcardially with 20 ml normal saline. The brains were removed from the skull and frozen immediately in isopentane (−20°C). Thick coronal cryosections (20 μm) were cut every 400 μm, and the sections were stained according to the silver staining protocol, scanned at 600 dpi and the infarct area on each section analysed (Scion Image). For the permanent coagulation model inducing exclusively cortical infarcts, the Swanson method (Swanson *et al*., 1990) was applied for indirect infarct measurement and correction for cortical swelling:

(Ischaemic area) = (Cortex area of the contralateral side)
− (Non-ischaemic cortex area of the ipsilateral side)

For the filament model (30 and 60 min occlusion) comprising also subcortical lesions, we used direct infarct measurement and corrected for brain oedema by subtracting the ipsilateral minus contralateral hemisphere area from the directly measured infarct area. The total infarct volume was determined by integrating measured areas and distances between sections.

Functional outcome test

The 'corner test' was performed (Zhang *et al*., 2002) to measure sensorimotor dysfunction at 24 h before middle cerebral artery occlusion (MCAO) and on Day 1, 3 and 7 after MCAO. Mice were placed between two boards set at a 30° angle and allowed to move freely. An observer blinded to treatment allocation counted left and right turns with a rearing movement after deep entry in the corner and calculated the ratio of right and left turns as an indicator of behavioural asymmetry. At least 12 full turns after a rearing movement were counted for each testing.

Immunohistology

We performed immunohistochemistry of mature T lymphocytes, B cells and neutrophilic granulocytes on coronal cryostat sections (12 μm) after pretreatment with 4% paraformaldehyde for 60 min. We blocked endogenous peroxidase with Peroxidase Blocking solution (Dako), then incubated the sections with primary antibodies against CD3 (Clone 3H698, Zytomed) or myeloperoxidase (Clone RP-053; Zytomed) for 60 min at 21°C. Immunoreactivity was visualized by a universal immunoenzyme polymer method (Nichirei Biosciences) and sections developed in diaminobenzidine. We investigated the distribution of activated microglia by immunohistochemical staining of coronal cryostat brain sections (12 μm) for IBA1 (Wako). Immunoreactivity was visualized by the avidin-biotin complex method and sections developed in diaminobenzidine. For immunofluorescence staining of von Willebrand Factor, VCAM-1 and CD3, sections were fixed in −20°C acetone for 10 min and then washed in phosphate buffered saline containing

0.1% Tween-20. After blocking with 10% goat serum for 1 h at room temperature, the sections were incubated with monoclonal rat anti-VCAM-1 (clone:99-12, Santa Cruz) and polyclonal rabbit anti-von Willebrand factor (Abcam) in blocking buffer at room temperature. The sections were then incubated with fluorochrome-conjugated secondary antibodies (Jackson ImmunoResearch) diluted 1:500 in blocking buffer for another 1 h at room temperature. Finally, the sections were thoroughly washed and then mounted on coverslips. For analysis of cell number, we captured the images on a Zeiss Axiovert 200M microscope. Blinded samples were evaluated for absolute cell counts by three individual analysers (A.L., W.Z. and A.H.D.), uninformed about treatment groups. One complete ischaemic hemisphere per mouse was analysed on coronal sections at the anterior commissure position by consecutive high power field analysis for the presence of positively stained cells. All images for the analysis of IBA1$^+$ cell numbers were processed with the TissueQuest software (TissueGnostics) for cell-based counting of automatically recognized IBA1$^+$ cells in a fluorescence activated cell sorting (FACS)-like manner of scattergram analysis (Ecker *et al*., 2006; Liesz *et al*., 2009*b*). Non-specifically stained structures and objects that were too large were excluded from the analysis.

Isolation of brain-invading leukocytes

We perfused the mice transcardially with 20 ml normal saline and removed the brains immediately from the skull. We split the hemispheres, mechanically homogenized the tissue after incubation in dissociation buffer (10 ml RPMI-1640, 180 units collagenase IV, 250 units DNase), and overlaid the cell suspension on Percoll gradients of 1.03 and 1.088 g/ml density. The collected mononuclear cells from the interphase were processed for flow cytometry.

Flow cytometry

We collected organs (spleen, blood and brain) after transcardial perfusion with saline at various time points after MCAO for flow cytometric analysis. We employed a modified version of previously published protocols (Gelderblom *et al*., 2009; Liesz *et al*., 2009*b*) for quantitative FACS analysis of lymphocytes infiltrating the brain. The respective single cell suspensions were stained for anti-mouse CD3 (Clone 17A2), CD4 (Clone RM 4-5), CD25 (Clone 7D4), Foxp3 (Clone FJK-16s), B220 (Clone RA3-6B2), NK1.1 (Clone PK136), Gr-1 (RB6-8C5), CD11b (Clone M1/70) and the appropriate isotype control by following the manufacturer's protocols (eBioscience). We performed flow cytometry on a Becton Dickinson FACS Calibur and analysed the data by CellQuest Pro software. Gates were set according to unstained samples and isotype control; compensation was adjusted using BD CaliBRITE Beads (BD Bioscience). We used quantitative calibration with the BD QuantiBRITE PE Beads (BD Bioscience) for flow cytometric quantification of CD49d expression on peripheral leukocytes and absolute leukocyte counts in brain homogenates. We performed intracellular FACS analysis of IFN-γ expression in CD3$^+$ cells, as previously described (Liesz *et al*., 2009*b*). In brief, splenocytes of naïve mice were primed for 48 h with CD3- and CD28-specific antibodies and increasing concentrations of either CD49d-specific antibodies or control antibodies. Then, we restimulated cells for 5 h with ionomycin, phorbol myristate acetate and Brefeldin and stained the cells for extracellular CD3 and intracellular IFN-γ expression after cell permeabilization.

RNA isolation and real-time polymerase chain reaction

We isolated RNA from separated cerebral hemispheres and from peripheral blood mononuclear cells using the RNeasy kit (Qiagen). Reverse transcription was performed with the High Capacity complementary DNA Archive Kit (Applied Biosystems) and real-time polymerase chain reaction with SYBR-Green assays (Applied Biosystems) on an ABI7500 real-time polymerase chain reaction System (Applied Biosystems). Primers were purchased as ready-to-use primer sets for each gene (Super Array). All assays were run in duplicate. We normalized the results for each individual gene to the level of the housekeeping gene encoding for peptidylprolyl isomerase A (cyclophilin) for brain samples and to actin-β for peripheral blood mononuclear cell samples.

Streptococcus pneumoniae infection and analysis of bacterial load

Refer to the Supplementary Material for detailed descriptions of procedures.

Cytokine enzyme-linked immunosorbent assay

Serum was collected and frozen at -80°C immediately until analysis of cytokine protein concentrations with commercial kits for the quantitative assay of INF-γ, IL-10 (all from R&D Systems), TGF-β, IL-6 and TNF-α (eBioscience).

Depletion of leukocyte subpopulations

Cell population specific depletion was performed by intraperitoneally injecting the respective antibody diluted in sterile phosphate buffered saline. All antibodies were purchased from eBioscience. Effectiveness and specificity of the depletion was controlled by complete blood cell counting at the Core Laboratory Facilities at the University of Heidelberg and by flow cytometric analysis of lymphocyte subpopulations. Granulocyte-specific depletion: 400 μg functional grade purified rat anti-mouse Gr-1, clone RB6-8C5. Cytotoxic T cell-specific depletion: 300 μg functional grade purified rat anti-mouse CD8a (Ly-2), clone 53-6.7. T helper cell-specific depletion: 300 μg functional grade purified rat anti-mouse CD4 (L3T4), clone GK1.5.

Intracerebroventricular injection

Mice were anaesthetized with 1.0–2.0% halothane in O_2/N_2O enriched air and fixed in a stereotactic frame (Stoelting). After making a midline incision in skin over the skull, a 10 μl Hamilton syringe was used for intracerebroventricular drug administration at 0.9 mm lateral, 0.1 mm posterior and 3.1 mm deep relative to the bregma. We injected either 1 μg neutralizing antibodies against mouse IFN-γ (Clone XMG1.2, eBioscience) or control antibodies diluted in 2 μl artificial cerebrospinal fluid consisting of, in mM: 126 NaCl; 2.5 KCl; 1.2 NaH2PO4; 1.3 MgCl2 and 2.4 CaCl2 at pH 7.4.

VCAM-1 micro-western blotting

Brain tissues of infarcted and non-infarcted hemispheres were separately scraped off with a scalpel from 20 μm thick coronal cryosections every 400 μm through the infarcted brain area at room temperature

and homogenized in ice-cold radioimmune precipitation buffer [50 mM Tris–HCl pH 7.5, 150 mM NaCl, 1% NP-40, 1% sodium deoxycholate, 1mM PMSF, 1mM EDTA and 10% Protease Inhibitor Cocktail (Sigma Aldrich)]. After centrifugation at 13 000 rpm for 10 min at 4°C, the supernatant was collected and the protein concentration of each sample was determined in triplicate using Bradford reagent. Aliquots of lysates containing 50 μg protein underwent electrophoresis on 8% sodium dodecyl sulphate polyacrylamide gels and then were transferred to nitrocellulose membranes. After blocking in 5% non-fat milk in Tris-buffered saline containing 0.1% Tween-20 for 1 h, blots were incubated overnight at 4°C with monoclonal rat anti-VCAM-1 (clone 99-12, Santa Cruz). Peroxidase-conjugated goat anti-rat antibody was used as secondary antibody and blots were detected using a standard chemical luminescence method. Sol8 cell lysate (Santa Cruz) was used as positive control. Blots were stained with rabbit anti-actin antibody (Sigma Aldrich) to confirm equal loading and transfer.

Micro-polymerase chain reaction

Brain tissue was collected as described above for micro-western blotting and processed by syringe-and-needle homogenization in lysis reagent. The RNA was then isolated using an RNeasy® Micro kit (Qiagen) and we applied the standard real-time polymerase chain reaction protocol described above, modified to meet the reduced RNA amount.

Fluorescence spectroscopy

Naïve mice were treated i.p. with 1 mg/kg or 15 mg/kg body weight of either unconjugated or fluorescein isothiocyanate-conjugated VCAM-specific antibodies (clone: 429, eBioscience). Then, 24 h after antibody treatment, mice were sacrificed and fresh brain tissue was homogenized in ice-cold RLT buffer (Qiagen). Brain homogenates were analysed in black 96-well plates on a Synergy4 monochromatic detection system (BioTek). Excitation of the samples was at 518 nm and emission spectrum detected from 520–700 nm in 1 nm steps; RLT lysis buffer in the final concentration was used as standard control for calibration. All samples were analysed in triplicate.

VCAM-1 gene silencing

In vivo silencing of VCAM-1 was performed by hydrodynamic injection of small interfering RNA into the femoral vein as previously described (Hino *et al*., 2006; Herweijer and Wolff, 2007). The left femoral vein was dissected and freshly diluted small interfering RNA in 1 ml RNase-free water injected through a microcatheter into the vein within 5 s. After injection, the catheter was left in place under compression until haemostasis. The treatment group received 30 nmol VCAM-1 Silencer® Select small interfering RNA, *in vivo* ready, per mouse (~16 mg/kg body weight), control animals received 30 nmol Silencer® Select Negative Control #1 small interfering RNA, *in vivo* ready (all small interfering RNA was commercially purchased from Ambion). Mortality induced by this procedure was <5%.

Statistical analysis

All values in bar graphs are expressed as mean ± standard deviation (SD). We analysed infarct volumes and functional outcome tests by two-tailed Student's *t*-test between two groups and ANOVA for multiple comparisons with *post hoc* Tukey's test, respectively, after validating the normal distribution of these data sets (Kolmogorov–Smirnov test). Log rank test was used to compare survival curves. For the remaining data, we used two-tailed Wilcoxon rank-sum test for comparison between two groups; for three and more groups we applied the Kruskal–Wallis H test with Dunn's *post hoc* testing, using GraphPad Prism 5 software. $P < 0.05$ was considered statistically significant.

Results

Integrin α4 inhibition improves experimental stroke outcome

We analysed the effect of blocking the α4-integrin (CD49d) on leukocytes on infarct volume after experimental ischaemia by intraperitoneal administration of 300 μg CD49d-specific monoclonal antibodies. Unless otherwise stated, MCAO was induced by permanent trans-temporal coagulation of the left middle cerebral artery distal to the lenticulostriate arteries that results in moderately sized cortical infarcts. By administering anti-CD49d 24 h before MCAO, infarct volumes at 7 days were significantly lower compared with control treatment with IgG2 isotype antibodies (Fig. 1A), but no differences in infarct volume were observed between treatment groups at 24 h MCAO (Fig. 1A), indicating that CD49d blockade mainly affected delayed damage. Blocking CD49d 3 h after MCAO resulted in a similar therapeutic effect (Fig. 1B). Furthermore, anti-CD49d treatment also improved behavioural outcome after permanent MCAO as tested by the corner test detecting sensorimotor asymmetry (Zhang *et al*., 2002). Mice in both groups deviated from the normal ratio of 1.0 towards an increased right-turn ratio at 24 h after MCAO, but mice in the anti-CD49d treated group recovered significantly earlier and more pronounced 3 and 7 days after MCAO than those in the control group (Fig. 1C). We additionally validated this therapy in a model of reversible filament-induced MCAO with 30 and 60 min occlusion time, respectively. Occlusion for 30 min resulted in moderate striatal lesions that were significantly reduced by CD49d-inhibition (Fig. 1D). In contrast, transient MCAO for 60 min induced extensive lesions, encompassing ~50% of one hemisphere (Fig. 1E). We did not detect a significant difference in infarct volume between treatment groups in mice undergoing these extensive lesions, however, mortality at 7 days in this model exceeded 40%, precluding conclusive comparison of infarct size (Dirnagl, 2006) (Fig. 1F). Survival did not significantly differ between groups [$P = 0.063$, $n = 23$ (IgG2), $n = 20$ (anti-CD49d), four individual experiments].

The lesion volumes 7 days after MCAO in the permanent coagulation and 30 min occlusion model were reduced as a result of a consistent decrease in infarct expansion throughout the complete infarct range rather than decrease in a specific anatomical area (Fig. 1G).

Anti-CD49d treatment inhibits cerebral leukocyte invasion

The therapeutic effect of anti-CD49d therapy in primary inflammatory diseases is believed to be mainly mediated by inhibiting lymphocyte migration (Engelhardt and Kappos, 2008).

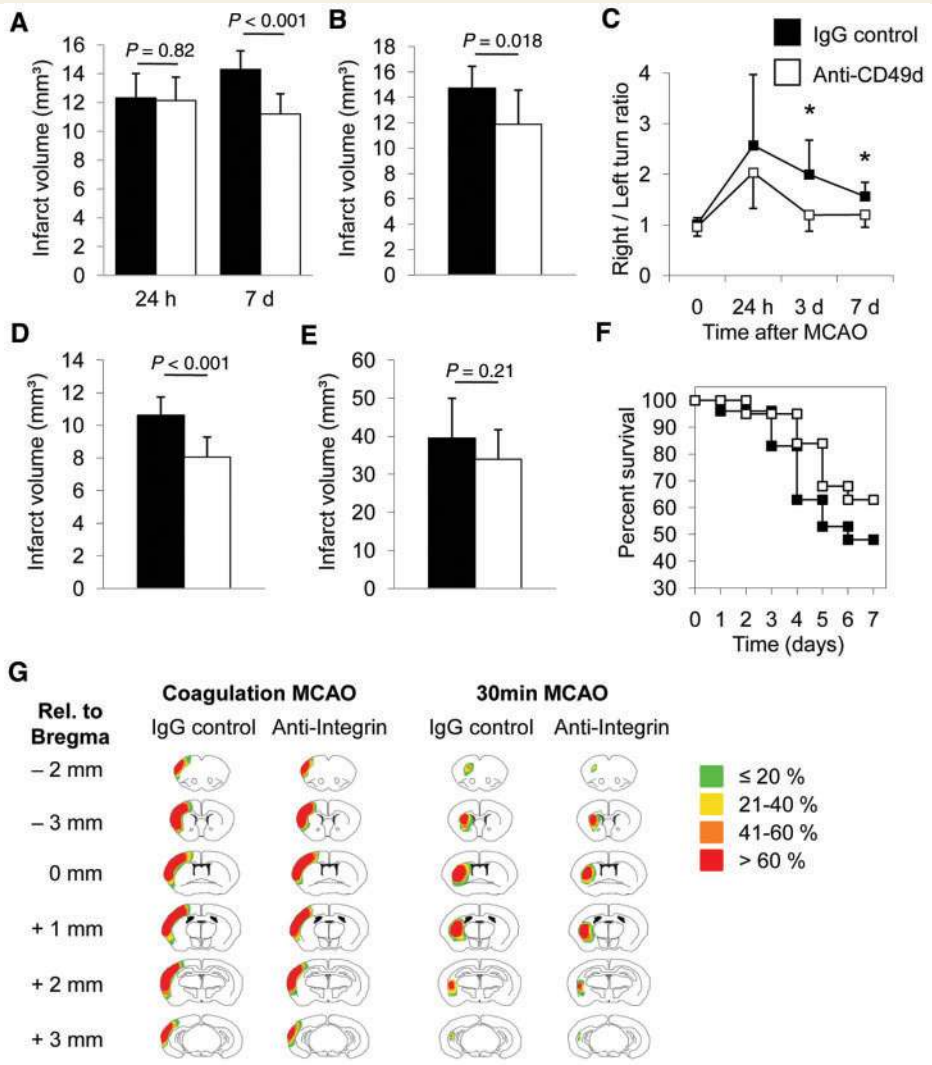

Figure 1 Anti-CD49d treatment improves stroke outcome. (**A**) Infarct volume 7 days after permanent MCAO, 24 h after i.p. injection of IgG2 control antibodies or CD49d-specific monoclonal antibodies ($n = 10$ per group, two individual experiments). (**B**) Infarct volumes 7 days after MCAO and antibody administration 3 h after MCAO ($n = 10$ per group, two individual experiments). (**C**) Behavioural dysfunction was determined using the 'corner test' for sensorimotor asymmetry. *$P < 0.05$ between treatment and control groups ($n = 10$ per group, two individual experiments). Infarct volumes were also determined 7 days after MCAO in (**D**) 30 min ($n = 10$ per group, two individual experiments) and (**E**) 60 min ($n = 11$ per group, three individual experiments) reversible ischaemia-reperfusion models. (**F**) Survival of mice after 60 min reversible ischaemia was assessed during 7 days after MCAO. (**G**) Schematic distribution of infarcted brain tissue 7 days after permanent MCAO by transcranial coagulation or 30 min transient MCAO. Each slide depicts the accumulated information about infarct density (colour coded as indicated) of 10 brains per group at the given coronal section in relation to the bregma.

Immunohistochemical study of brain sections for T cells, B cells and granulocytes (Fig. 2A) revealed that invading leukocytes were predominantly located in the peri-infarct zone 5 days after permanent MCAO, as previously reported (Liesz *et al*., 2009*b*). One total section per brain was analysed for the presence of positively stained leukocytes. Brain invasion of T and B cells was negligible at 24 h but became apparent at 5 days. Anti-CD49 treatment significantly reduced lymphocyte infiltration at Day 5 (Fig. 2B). Myeloperoxidase positive granulocytes invaded the brain already 24 h after MCAO and further increased 5-fold until Day 5. Granulocyte invasion was significantly attenuated by the therapy at both time points (Fig. 2B).

Since our previous work suggested a strong post-ischaemic interaction between invading leukocytes and microglial cells, we measured the number of activated (IBA1$^+$) microglia/monocytes (Fig. 2C). Twenty-four hours after permanent MCAO, no difference could be observed for IBA1$^+$ cell counts between treatment groups in both hemispheres. In contrast, 5 days after ischaemia, anti-CD49d significantly reduced the number of IBA1$^+$ cells in the ischaemic hemisphere, suggesting that reducing leukocyte invasion subsequently attenuates the activation of resident (migroglia) or invading (monocytes) innate immune cells, respectively. We further differentiated the effect of anti-CD49d treatment on subpopulations of brain invading leukocytes by flow cytometry. Cells of

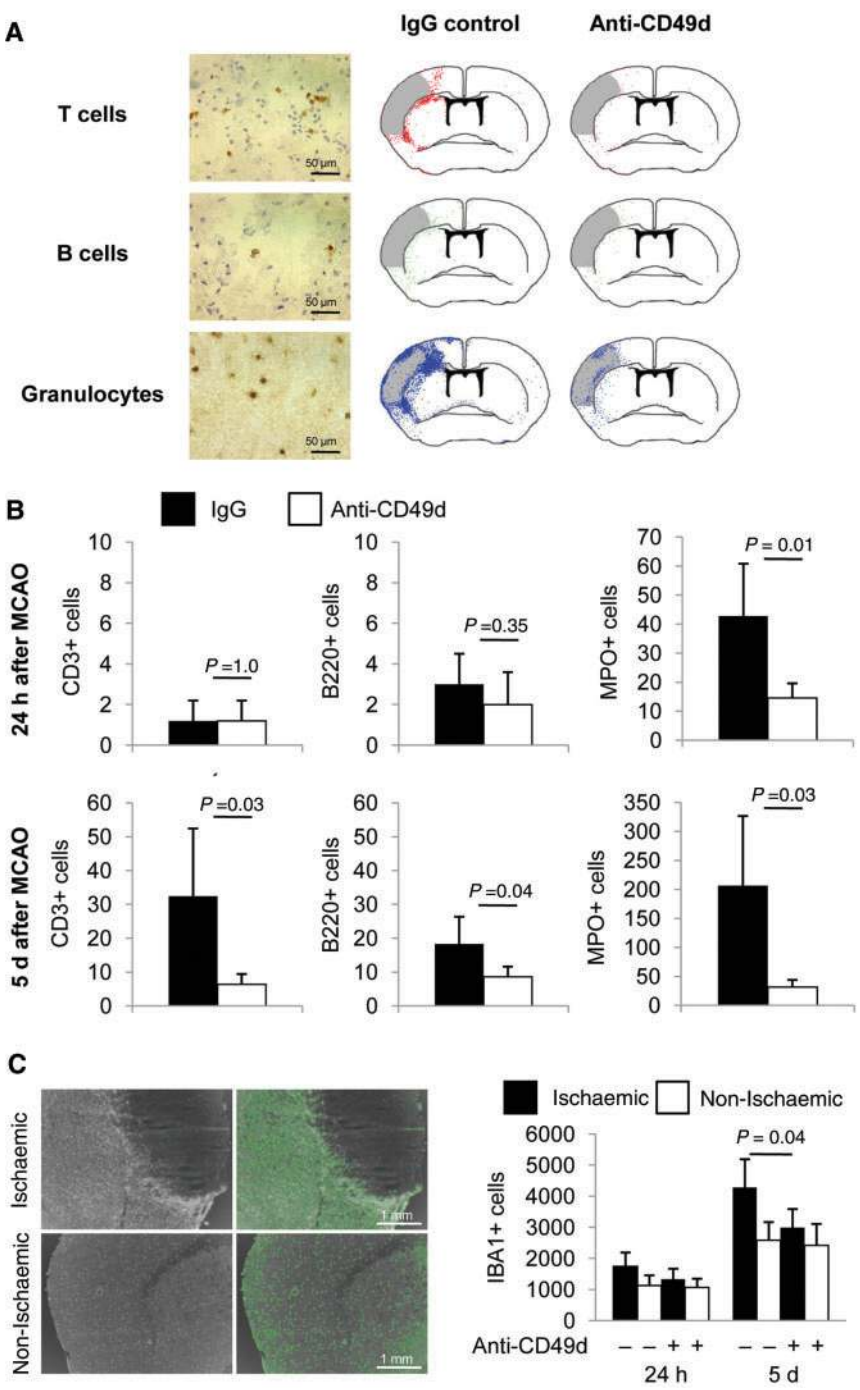

Figure 2 Anti-CD49d treatment inhibits leukocyte migration into the ischaemic brain. (**A**) Representative, immunohistochemically stained sections for T cells (CD3), B cells (B220) and granulocytes (myeloperoxidase) 5 days after MCAO and corresponding topographic map of five accumulated brain sections. (**B**) Analysis of T cell, B cell and granulocyte counts per one complete section of the ischaemic hemisphere 24 h and 5 days after MCAO ($n = 8$ per group, two individual experiments). (**C**) Representative images used for cell-based scattergram analysis of activated microglia/monocytes (IBA1$^+$; *left*: original images, *right*: automated cell identification) and corresponding data for IBA1$^+$cell counts per one complete section of the ischaemic and non-ischaemic hemisphere in both treatment groups 24 h ($n = 5$) and 5 days ($n = 10$, three individual experiments) after MCAO.

homogenized ischaemic hemispheres were gated for CD45$^+$ leukocytes and quantitative cell numbers of subpopulations were determined (Liesz *et al*., 2009*b*) (Fig. 3A). At 5 days after MCAO, cell counts of all populations were reduced by anti-CD49d. Interestingly, invasion of all T cell subsets including cerebroprotective regulatory T cells were similarly affected by anti-CD49d treatment (Fig. 3B). These results are consistent with a broad effect of α4-integrin inhibition on the migratory capability of all analysed

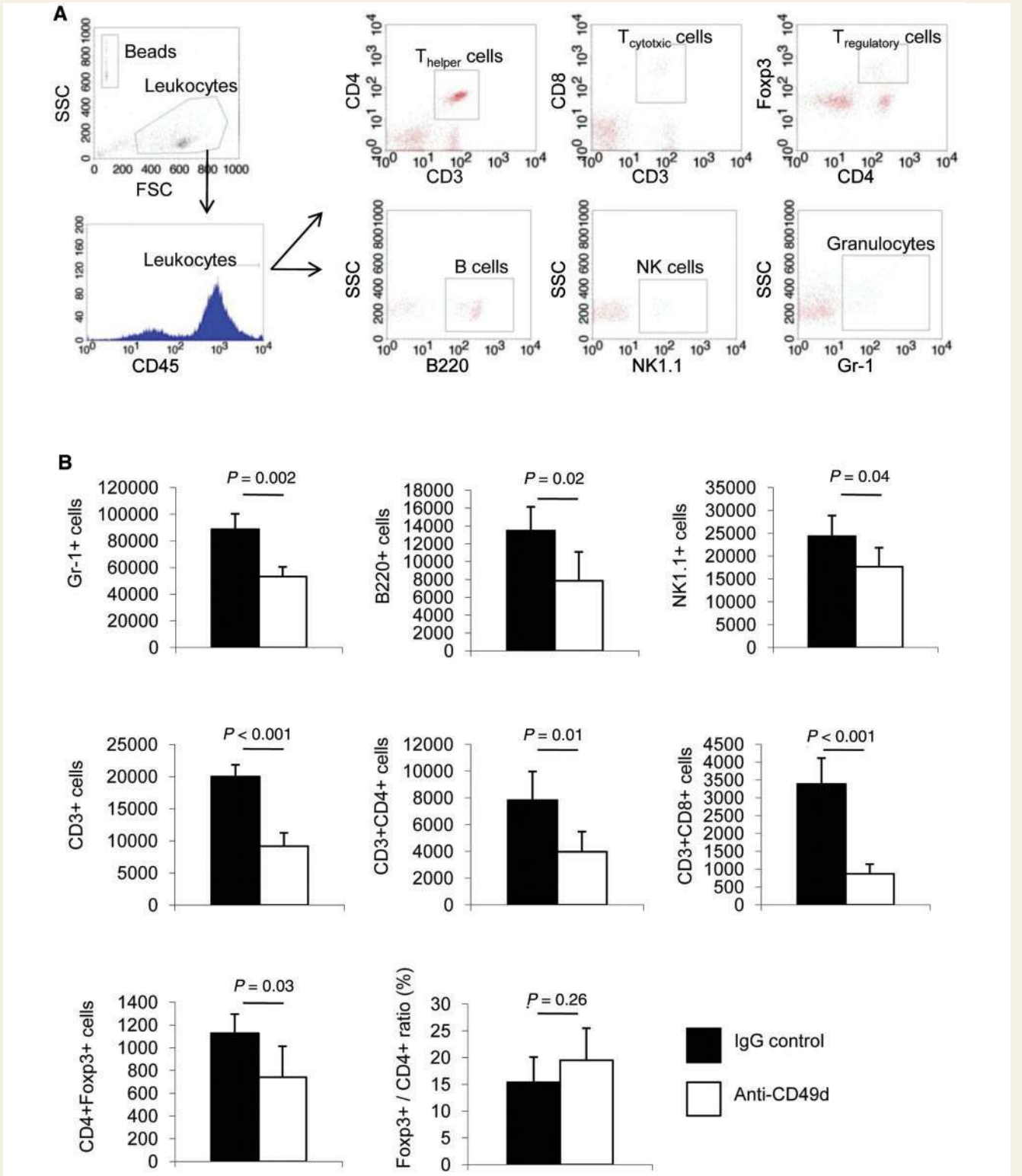

Figure 3 Anti-CD49d treatment reduces leukocyte brain invasion. (**A**) Representative gating strategy for absolute cell count analysis of leukocyte subpopulations in ischaemic hemisphere homogenates. $CD45^+$ leukocytes were gated for subpopulation analysis after using a scattergram gate for viable leukocytes and quantification beads. (**B**) Flow cytometric analysis of absolute cell counts for granulocytes ($Gr\text{-}1^+$), B– ($B220^+$), NK- ($NK1.1^+$), total T cells ($CD3^+$) and T_{helper}- ($CD3^+CD4^+$), $T_{cytotoxic}$- ($CD3^+CD8^+$), regulatory T cells ($CD4^+Foxp3^+$), and the ratio of regulatory T cells within the T_{helper} population 5 days after MCAO in IgG2 control treated and anti-CD49d treated animals (five individual experiments per group, consisting of 2–3 pooled animals each) SSC = side scatter.

leukocyte populations rather than on specific pro-inflammatory cells only.

Anti-CD49d treatment attenuates expression of specific cerebral cytokines

We investigated the impact of anti-CD49d treatment on cerebral cytokine expression after permanent MCAO (Fig. 4). The messenger RNA levels of the proinflammatory cytokines IFN-γ and IL-6 were significantly reduced in anti-CD49d treatment groups at their expression maximum 3 days after MCAO, compatible with the time course of lymphocyte invasion (Gelderblom *et al*., 2009). We did not detect a difference in the expression of IFN-γ at 24 h, however, the cellular source for its increase in the ischaemic hemispheres of both treatment groups at this early time point before lymphocyte invasion remains unclear. In contrast, IL-1 and TNF-α, which we and others have previously shown to

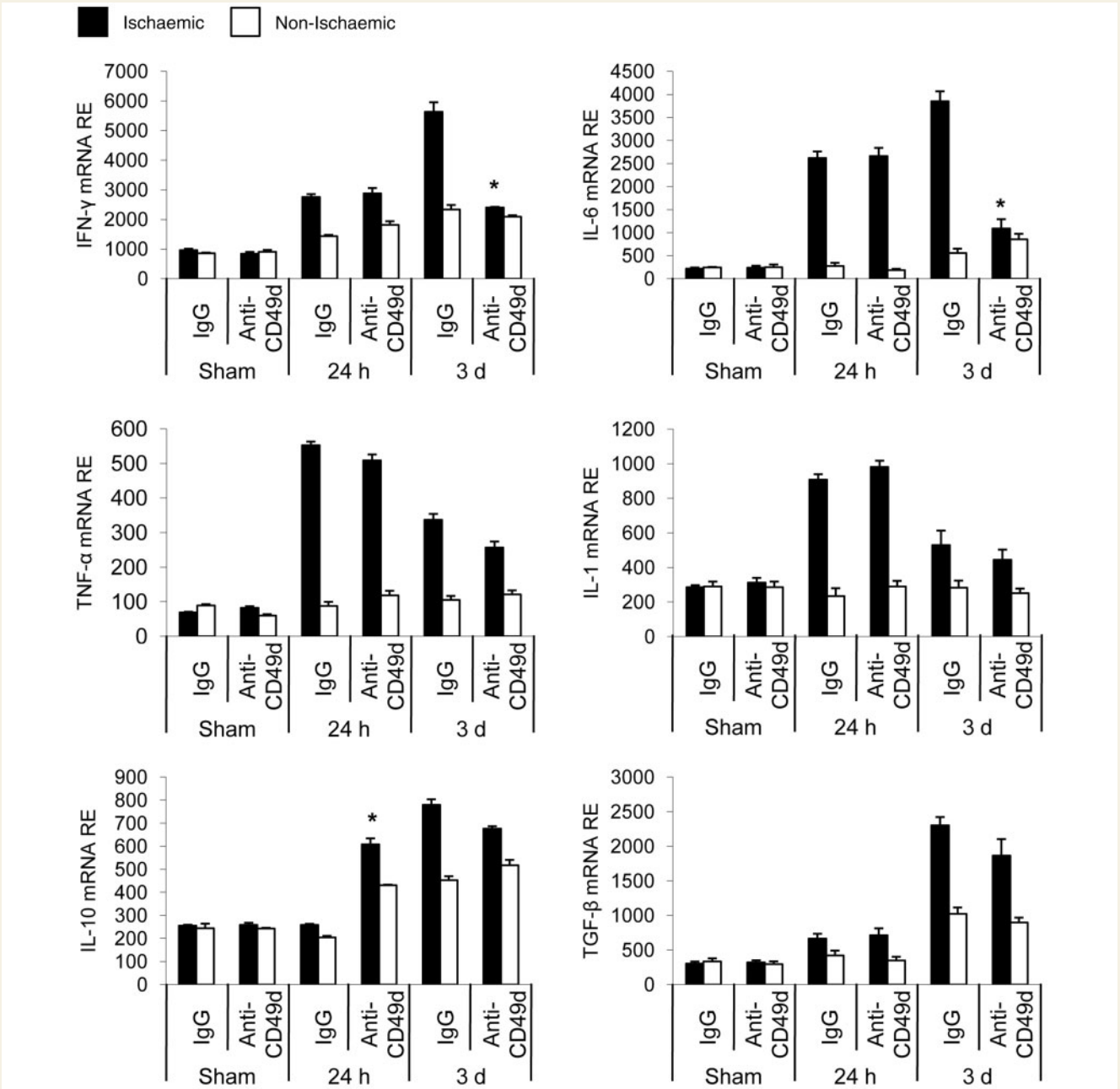

Figure 4 Anti-CD49d treatment reduces expression of key proinflammatory cytokines after MCAO. Cytokine messenger RNA relative expression (RE, normalized to peptidylprolyl isomerase A housekeeping gene) for pro-inflammatory (INF-γ, IL-6, TNF-α and IL-1) and anti-inflammatory (IL-10 and TGF-β) cytokines was measured by real-time polymerase chain reaction in the ischaemic and non-ischaemic hemispheres of control (IgG2) and anti-CD49d treated mice ($n = 5$ per group, 2–3 individual experiments per group). *$P < 0.05$ between ischaemic hemispheres of treatment and control groups at one respective time point.

be mainly produced by microglia after ischaemia (Davies *et al*., 1999; Lambertsen *et al*., 2005; Liesz *et al*., 2009*b*), was not influenced by the therapy. Analysis of the anti-inflammatory cytokines IL-10 and TGF-β yielded a transient increase of IL-10 in anti-CD49d treated animals compared with controls at 24 h but no difference at 3 days (Fig. 4).

Leukocytes ubiquitously express α4-integrin and remain functionally unaffected by anti-CD49d treatment

As most previous reports targeting α4-integrins in neuroinflammation were focused on lymphocyte-mediated effects (Yednock *et al*., 1992; Engelhardt and Kappos, 2008), we performed a comprehensive analysis of α4-integrin expression on leukocyte subsets. Cellular binding of the same CD49d-specific antibody clone used for *in vivo* blocking was measured on leukocyte subpopulations in naïve mice and after permanent MCAO. Conventional flow cytometric analysis revealed that a high percentage (68–99%) of all leukocyte subpopulations expressed α4-integrins constitutively (Fig. 5A). Interestingly, the absolute number of CD49d molecules detected per cell was comparatively low in naïve and post-ischaemic T cells while CD49d-specific antibody binding was substantially increased on granulocytes 24 h after MCAO compared with naïve granulocytes (Fig. 5B), in accordance with previous data for α4-integrin upregulation under conditions of strong immunological stimuli (Ibbotson *et al*., 2001). Furthermore, CD49d transcription of total peripheral blood mononuclear cells did not differ between control treatment and anti-CD49d treated animals and was similar at the analysed time points before and after MCAO (Fig. 5C), consistent with the concept of conformational regulation of α4-integrin rather than transcriptional regulation upon activation (Takagi and Springer, 2002).

We also performed differential blood cell counting to examine the effect of antibody-treatment on peripheral cell counts. Numbers of granulocytes, lymphocytes, monocytes and thrombocytes did not differ between anti-CD49d and control groups (Supplementary Fig. 1), nor did flow cytometric analysis reveal any differences for T_{Helper}-, $T_{Cytotoxic}$-, B_- and NK in blood from treatment and control groups (Supplementary Fig. 1). Since CD49d-specific antibodies have been reported to be potentially co-stimulatory (van Seventer *et al*., 1991; Damle *et al*., 1992), we investigated the activation of T cells as IFN-γ-expressing cells after *in vitro* stimulation with increasing antibody concentrations. Anti-CD49d did not alter the number of $CD3^+IFN\text{-}\gamma^+$ cells compared with controls at any concentration of CD49d-specific antibodies (Fig. 5D). Moreover, no significant alterations in IFN-γ, TNF-α, IL-6, IL-10 and TGF-β serum levels were detected between groups either in sham operated animals or 24 h and 5 days after MCAO (Supplementary Fig. 2).

Additionally, we tested whether anti-CD49d treatment compromises the antimicrobial host defence because bacterial infections are a common complication of stroke (Emsley and Hopkins, 2008) and CD49d blocking might be a potent immunosuppressant. Because the ischaemia model used in this study only rarely induces infections (Liesz *et al*., 2009*a*), we challenged mice with the nasal administration of *Streptococcus pneumoniae* 3 days after MCAO, which has been shown to induce experimental pneumonia (Stegemann *et al*., 2009). Twenty-four hours later, bacterial counts in nasopharyngeal lavage and lung homogenates did not differ significantly between treatment groups (Fig. 5E and F). Futhermore, we did not detect any differences in bacterial 16s RNA loads in lung homogenates between groups (Fig. 5G). None of the animals had bacteria in blood samples. Thus, anti-CD49d treatment did not exacerbate post-ischaemic bacterial infections.

T cells and their molecular mediators are the main effectors of post-ischaemic neuroinflammation

To verify the concept that the effect of anti-CD49d therapy is lymphocyte dependent (Yednock *et al*., 1992; Rose *et al*., 2002), we analysed the impact of α4-integrin blockade on infarct volumes in lymphocyte-deficient $Rag2^{-/-}$ mice (Fig. 6A). As previously reported (Yilmaz *et al*., 2006; Liesz *et al*., 2009*b*), infarct volumes in $Rag2^{-/-}$ were significantly smaller than in wild-type control animals on the same genetic background (C57BL/6). Importantly, CD49d-blocking failed to reduce infarct volumes in $Rag2^{-/-}$ mice. Adoptive transfer of 1×10^8 total splenocytes 7 days before MCAO in lymphocyte-deficient $Rag2^{-/-}$ reconstituted the peripheral lymphocyte compartment (Supplementary Fig. 3) and significantly increased infarct volume at 7 days after MCAO (Fig. 6B). This increase in infarct size was again reduced by anti-CD49d administration at 24 h prior to MCAO (Fig. 6B), indicating lymphocytes as the main functional target of anti-CD49d treatment. To identify which T lymphocyte subpopulation contributed to ischaemic damage, T_{helper} or $T_{cytotoxic}$ cells were depleted 24 h before ischaemia by specific antibodies (Fig. 6C). Depletion of T_{helper} or $T_{cytotoxic}$ cells significantly reduced infarct volume. In both T_{helper} and $T_{cytotoxic}$ depleted animals (Fig. 6E), anti-CD49d treatment failed to further decrease ischaemia size (Fig. 6E). In contrast, granulocyte depletion (Fig. 6D) 24 h prior to MCAO did not alter infarct volumes 7 days after ischaemia, compared with control animals (Fig. 6E). In these mice, the additional administration of anti-CD49d significantly reduced infarct sizes by a similar extent as in naïve mice.

Because the role of T-cell mediated tissue damage in cerebral ischaemia has been only partially characterized, we further examined two key effector mechanisms, IFN-γ secretion (Schroder *et al*., 2004; Yilmaz *et al*., 2006) and direct cell cytotoxicity via perforin release (Russell and Ley, 2002; Trapani and Smyth, 2002), respectively. Intracerebroventricular administration of neutralizing IFN-γ-specific antibodies was performed 3 days after MCAO (Liesz *et al*., 2009*b*), which significantly reduced infarct volumes at 7 days compared with control treatment (Fig. 6F). Adding anti-CD49d treatment to IFN-γ neutralization significantly improved infarct volumes compared with IFN-γ antagonization alone. We investigated the relevance of perforin-mediated pathways using perforin-deficient $Prf^{-/-}$ mice (Fig. 6G). Infarct volumes in $Prf^{-/-}$ mice were significantly smaller 7 days after MCAO than in wild-type control animals. Interestingly, anti-CD49d failed

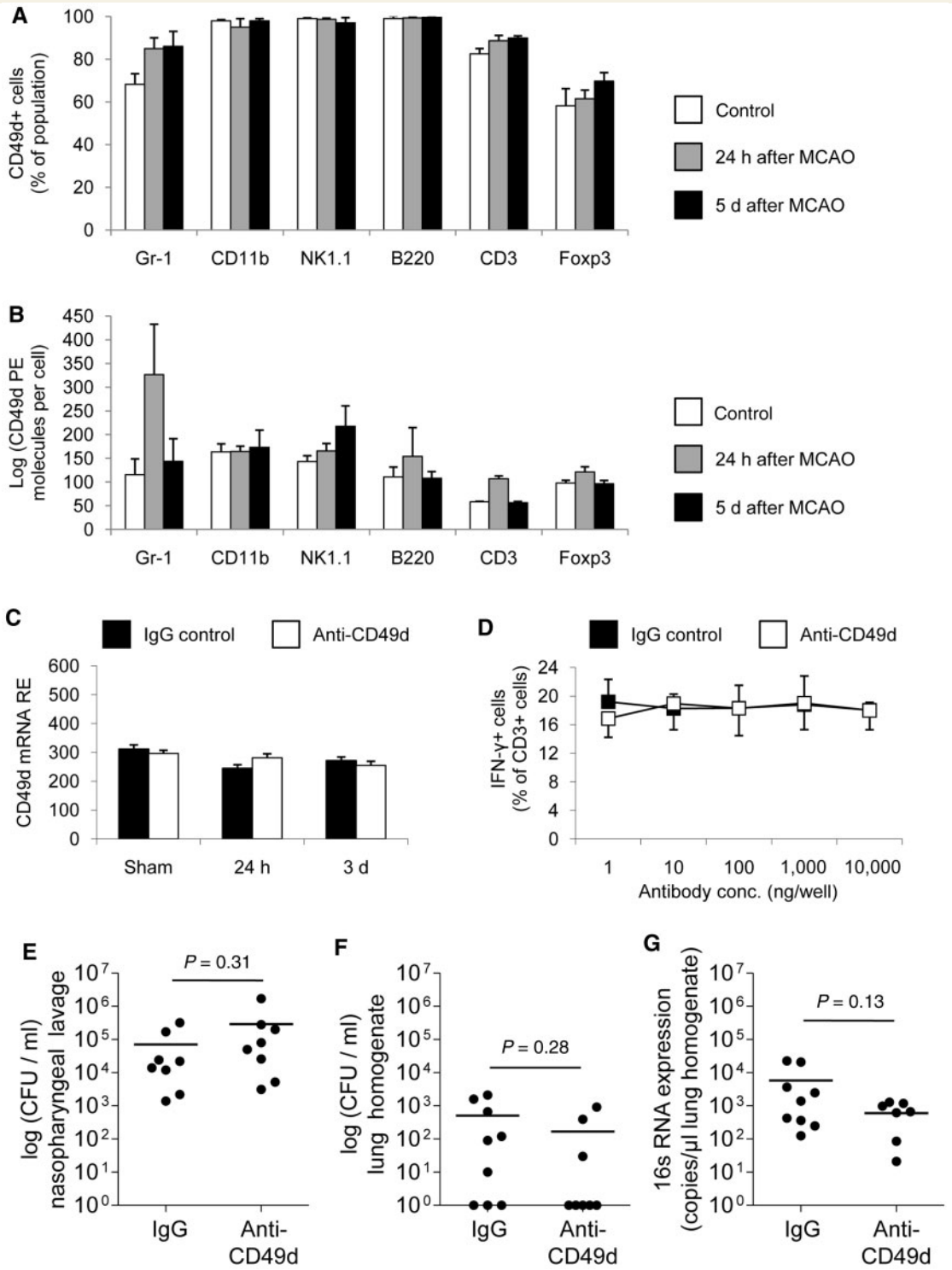

Figure 5 CD49d-specific antibodies bind to all leukocyte subpopulations but do not alter peripheral immune function. (**A**) Relative expression of CD49d and (**B**) the quantity of CD49d-specific antibodies bound per cell in the indicated cell populations, as measured by flow cytometry in naïve control animals and 24 h and 5 days after permanent MCAO ($n = 5$ from five individual experiments per group). (**C**) real-time polymerase chain reaction of CD49d messenger RNA expression in blood leukocytes after anti-CD49d or control treatment in Sham operated mice or 24 h and 5 days after MCAO ($n = 5$ per group, two individual experiments). (**D**) Lymphocyte stimulation by CD49d-specific antibodies compared with IgG2 treatment was determined by intracellular flowcytometric analysis of IFN-γ in $CD3^+$ cells after culture conditions with increasing amounts of antibodies per culture well (three individual experiments). Experimental pneumonia was induced in anti-CD49d or control treated animals 3 days after MCAO and 24 h later the number of colony forming units per ml of (**E**) nasopharyngeal lavage and (**F**) lung homogenates was measured. (**G**) Bacterial load was verified by polymerase chain reaction for bacterial 16s RNA expression per ml of lung homogenate. Dots represent individual mice and bars indicate mean values.

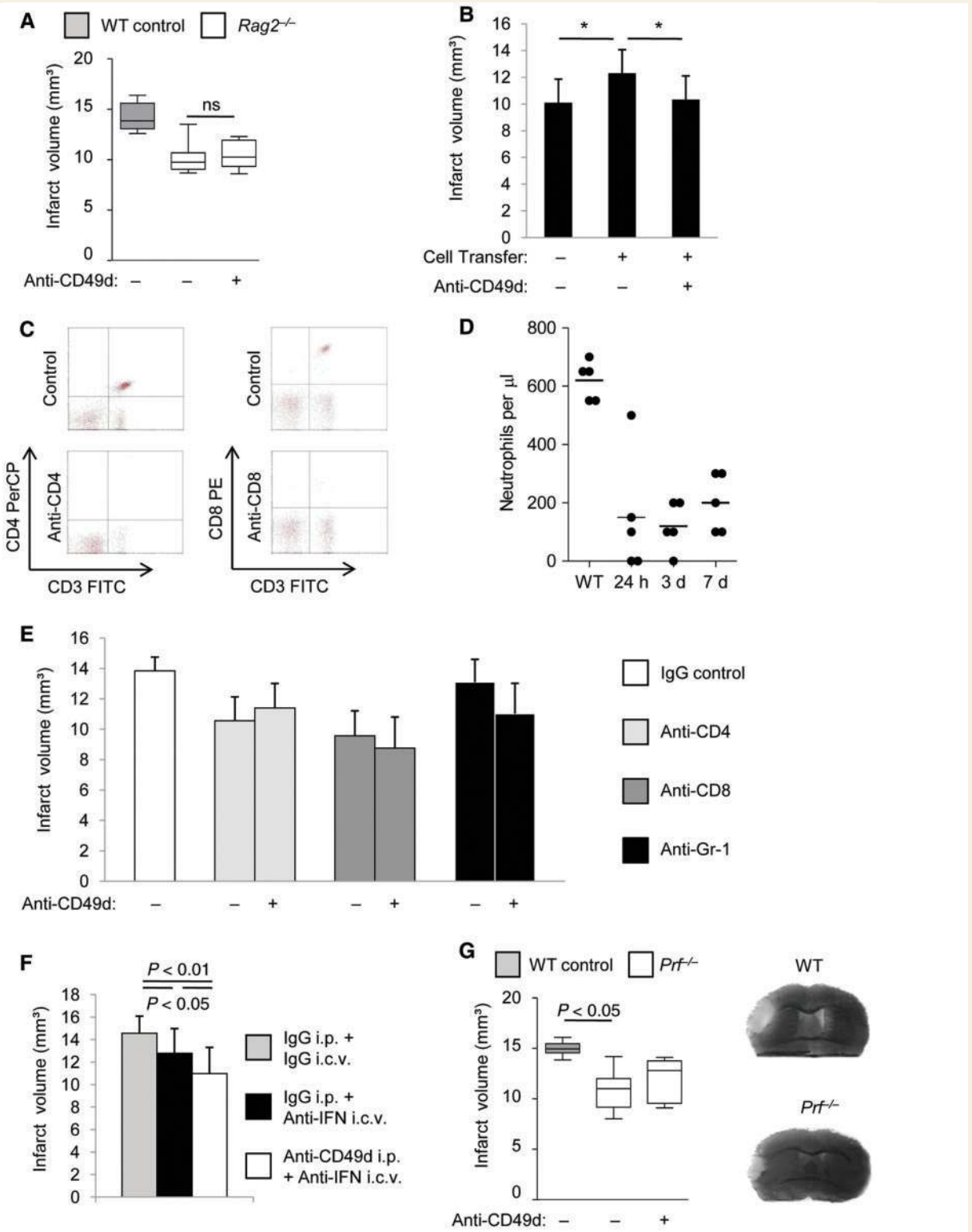

Figure 6 The neuroprotective effect of anti-CD49d is mediated via inhibition of T cell migration and abrogation of their key effector mechanisms. (**B**) Infarct volumes 7 days after MCAO in wild-type (WT) control mice and in lymphocyte-deficient *Rag2*$^{-/-}$ mice with IgG2 control or anti-CD49d treatment ($n = 10$ per group, two individual experiments). (**B**) *Rag2*$^{-/-}$ mice received adoptive transfer of 1×10^8 splenocytes 7 days prior to MCAO and infarct volumes were determined at 7 days after MCAO in IgG- or anti-CD49d-treated animals ($n = 15$ per group, three individual experiments). (**C**) T_{helper}- (anti-CD4) or $T_{cytotoxic}$- (anti-CD8) cells were depleted 48 h and mice treated 24 h before MCAO with IgG2 or CD49d-specific antibodies, infarct volumes were determined 7 days after infarct induction ($n = 10$ per group, two individual experiments). Representative dot plots are shown for depletion of the respective population and control treatment. (**D**) Neutrophil cell counts were determined by complete cell count analysis in control animals (WT) and 24 h, 3 days and 7 days after

(continued)

to reduce infarct volumes in these animals. In summary, these data underline the key pathophysiological role of invading T cells in post-ischaemic neuroinflammation.

Post-ischaemic VCAM-1 upregulation is inhibited by anti-CD49d treatment

We investigated the pathophysiological role of the main endothelial VLA-4 ligand VCAM-1 to further characterize integrin-dependent migration after ischaemia. In accordance with previous studies (Jander *et al*., 1996; Justicia *et al*., 2006), VCAM-1 was substantially upregulated with delay after MCAO (Fig. 7A). Intensively stained VCAM-1$^+$ vessels were primarily found in the peri-infarct vasculature. The invading CD3$^+$ T cells surrounded these VCAM-1$^+$ vessels, indicating a close association between lymphocyte invasion (compare Fig. 2A) and endothelial VCAM-1-induction in the peri-infarct area (Fig. 7B). Intriguingly, anti-CD49d treatment significantly inhibited the upregulation of VCAM-1 messenger RNA (Fig. 7C) and protein (Fig. 7D) in the ischaemic hemisphere. Thus, a dynamic crosstalk between leukocytes carrying activated α4-integrins and VCAM-1 expressing endothelial cells takes place after cerebral ischaemia (Cook-Mills and Deem, 2005; Hordijk, 2006).

Antibody-mediated blocking of VCAM-1 fails to improve ischaemia outcome

We attempted to block VCAM-1 by using monoclonal antibodies as an alternative target for inhibiting cerebral leukocyte invasion. Intraperitoneal injection of VCAM-1-specific rat-anti-mouse antibodies both 24 h before and 3 days after MCAO and staining for rat antibodies 6 days after MCAO revealed substantial binding of these antibodies to cerebral endothelial VCAM-1 (Fig. 7E). We further analysed the dose-dependent concentration of detectable VCAM-1-specific antibodies in brains 24 h after intraperitoneal injection. Administration of 300 μg FITC-labelled anti-VCAM-1 distinctly increased cerebral fluorescence as measured by spectrofluorometry and histology (Supplementary Fig. 4A and B), indicating effective binding at cerebral endothelium at the dosage (~15 mg/kg) used in the blocking experiments. Endothelial antibody binding was additionally shown by inhibiting secondary antibody adhesion to capillaries of treated animals (Supplementary Fig. 4C). However, despite using a substantially higher dose than previous investigators (Justicia *et al*., 2006) and repetitive administration 24 h before and 3 days after MCAO of monoclonal antibodies, anti-VCAM failed to reduce infarct volume 7 days after MCAO (Fig. 7F). Intriguingly, anti-VCAM antibodies did not significantly reduce cerebral invasion of neutrophils and T cells and did not affect cerebral IFN-γ expression either (Supplementary Fig. 5).

VCAM-1 gene silencing prevents cerebral leukocyte migration and reduces ischaemia size

Because the anti-VCAM antibody used in our experiments failed to inhibit leukocyte migration sufficiently, we studied another therapeutic paradigm for inhibiting VCAM-1-mediated leukocyte immigration. Here, hydrodynamic *in vivo* administration (Hino *et al*., 2006; Herweijer and Wolff, 2007) of VCAM-1 small interfering RNA significantly reduced VCAM-1 protein expression 5 days after MCAO by >65% compared with mice receiving a control small interfering RNA (Fig. 7G). We controlled the specificity of VCAM-1 silencing by real-time polymerase chain reaction analysis of VCAM-1 messenger RNA and the housekeeping genes in both hemispheres (Supplementary Fig. 6A–C). VCAM-1 silencing significantly reduced infarct volumes 6 days after MCAO compared with control small interfering RNA treatment (Fig. 7H). Further anti-CD49d treatment had no additional effect on infarct size, suggesting that VCAM-1 is the main complementary endothelial ligand for post-ischaemic leukocyte migration via VLA-4. VCAM-1 silencing significantly reduced cerebral granulocyte and T cell numbers 6 days after MCAO (Fig. 7I) and reduced IFN-γ expression to barely detectable levels (Supplementary Fig. 6D).

Discussion

Primary neuroinflammatory diseases share many inflammatory pathways with neurodegenerative, traumatic and vascular brain disorders that open new opportunities for translation of therapeutic concepts between aetiologically diverse disorders such as multiple sclerosis and stroke (Zipp and Aktas, 2006). Recent studies have shown that different T cell subpopulations have the capability to either contain or moderately exacerbate ischaemic brain damage suggesting that T cell-targeted therapy may be a promising new protective approach for stroke (Liesz *et al*., 2009*b*; Shichita *et al*., 2009). T cell trafficking into the brain parenchyma represents a key step of neuroinflammation in experimental allergic encephalomyelitis, the preclinical model of multiple sclerosis. Intriguingly, recent insights into the brain invasion of encephalitogenic T cells have confirmed the key role of the VLA-4–VCAM-1 axis in this process, which is consistent with the outstanding

Figure 6 Continued
granulocyte depletion with Gr-1-specific monoclonal antibodies. Dots represent individual mice and bars indicate mean values. (**E**) Infarct volumes 7 days after depletion of neutrophils or control treatment and in mice receiving depleting antibodies and additional blocking of CD49d (n = 10 per group, two individual experiments). (**F**) Infarct volumes 7 days after MCAO (n = 20 per group, four individual experiments) in mice receiving intracerebroventricular injection of control IgG antibody or neutralizing IFN-γ specific antibodies in artificial cerebrospinal fluid and additional administration of control IgG or CD49d-specific antibodies intraperitoneally (i.p.). (**G**) Infarct volume 7 days after MCAO in wild-type mice and in perforin-deficient *Prf*$^{-/-}$ mice with intraperitoneal injection of either IgG control or CD49d-specific antibodies 24 h before ischaemia induction (n = 10 per group, two individual experiments).

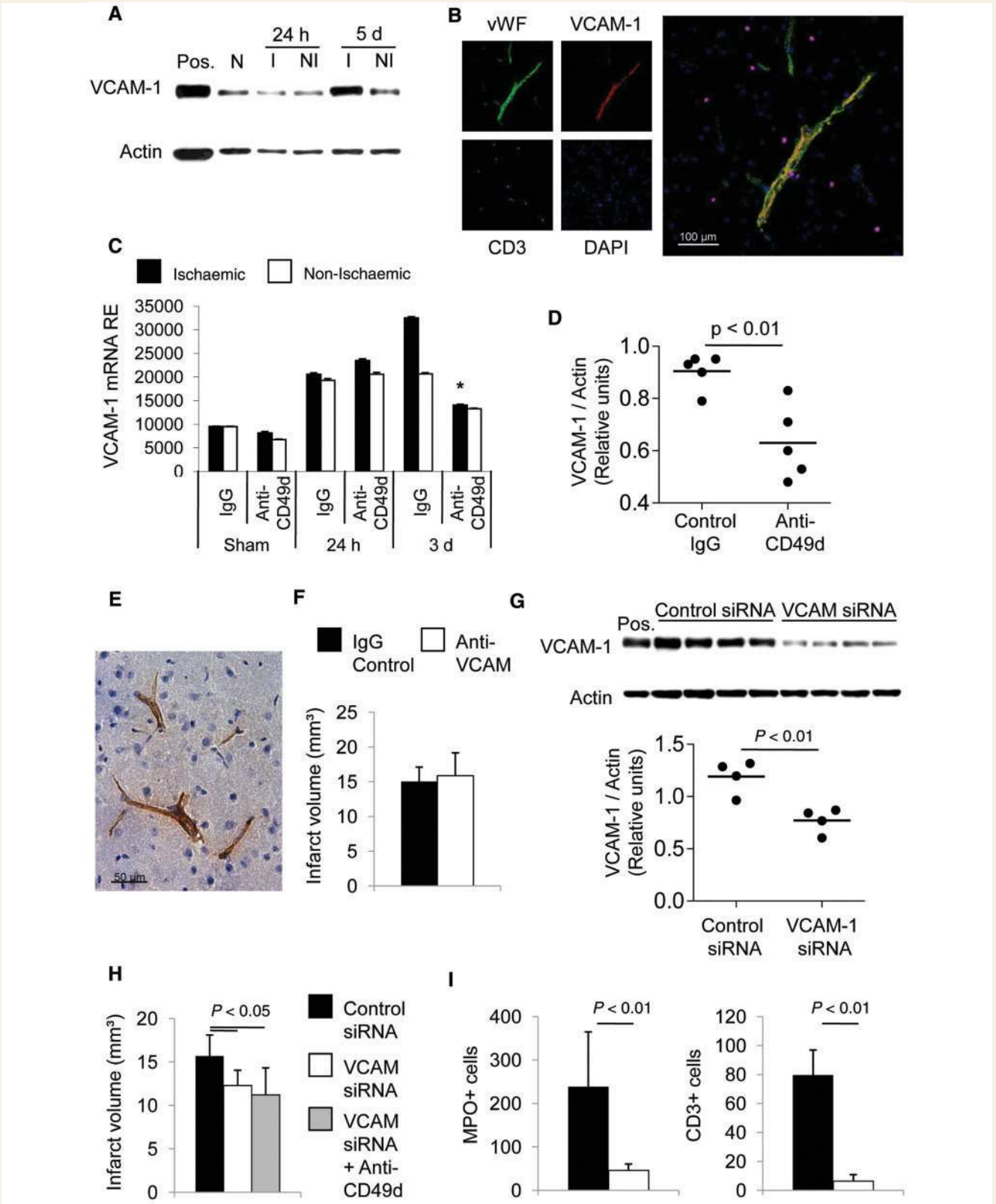

Figure 7 VCAM-1 is the principal endothelial CD49d-ligand for post-ischaemic leukocyte migration. (**A**) Representative micro western blot for VCAM-1 expression of ischaemic (I) and non-ischaemic (NI) hemispheres, in normal wild-type mice (N) and at 24 h and 5 days after MCAO. Actin was used as loading control. Representative image of five individual experiments. (**B**) Representative immunofluorescence staining for VCAM-1, von Willebrand Factor (vWF), T cells (CD3) and nuclei (DAPI) at 5 days after permanent MCAO. (**C**) Relative expression (RE) of VCAM-1 messenger RNA levels of control animals and anti-CD49d treated animals (24 h prior to ischaemia) after Sham operation and at 24 h and 3 days after MCAO (three individual experiments of 4–5 mice per group). (**D**) Densitometric analysis

(continued)

efficacy of its therapeutic blockade in multiple sclerosis (Yednock *et al*., 1992; Laschinger and Engelhardt, 2000; Steinman, 2005; Bartholomaus *et al*., 2009).

Using different models of permanent and transient cerebral ischaemia, we found that antibody-mediated blockade of α4-integrin reduces infarct size and improves behavioural outcome 7 days after moderate ischaemia. Although at first glance these results appear to be consistent with the beneficial effect reported in two small previous studies (Becker *et al*., 2001; Relton *et al*., 2001), outcome in these studies was measured at 24 and 48 h after MCAO, respectively, when no protection was observed in our experiments. Remarkably, at this early time point, lymphocytes—the key effector cells under these circumstances (see below)—have not yet started to invade the ischaemic brain (Jander *et al*., 1995; Gelderblom *et al*., 2009; Liesz *et al*., 2009*b*).

Because the mechanisms behind the protective effect of CD49d-blockade in cerebral ischaemia were so far unknown, we performed a comprehensive analysis of the complex interactions in transendothelial leukocyte migration and the pathogenic role of lymphocyte subpopulations. Although VLA-4 blocking by specific antibodies in multiple sclerosis is primarily perceived as a lymphocyte adhesion blocker (Rice *et al*., 2005), the profound reduction of post-ischaemic brain infiltration by α4-integrin or VCAM-1 blockade in our experiments was not restricted to a particular inflammatory cell type. Correspondingly, constitutive α4-integrin expression was present on the surface of most leukocytes. However, despite the non-specific reduction of inflammatory cell infiltration, the cerebroprotective effect was clearly mediated via inhibition of T cells. First of all, protection by CD49d-specific antibodies persisted in mice depleted of neutrophils, indicating a minor role of granulocytes in the immunopathology after stroke, although their role in post-ischaemic inflammation is still controversial (Schurer *et al*., 1991; Matsuo *et al*., 1994; Harris *et al*., 2005). In contrast, anti-CD49d treatment did not reduce infarct size in lymphocyte-deficient *Rag2*$^{-/-}$ mice and was ineffective after selective antibody-mediated depletion of either T_{helper} or $T_{cytotoxic}$ cells. Therefore, CD49d-targeted blockade can be regarded as a mainly T cell-targeted therapy although an indirect effect on the activation or recruitment of other cell populations (e.g. microglia) by the absence of cerebral lymphocytes cannot be excluded.

Beyond demonstrating the effectiveness of blocking the VLA-4–VCAM-1 axis, our study provides important insights into the functional role of T cells in cerebral ischaemia. In the absence of T lymphocytes or their subsets, infarct volumes have been smaller than in respective controls in several studies, including the present (Yilmaz *et al*., 2006; Hurn *et al*., 2007; Shichita *et al*., 2009; Kleinschnitz *et al*., 2010). Furthermore, antagonizing IFN-γ, a key cytokine of T cells, protected the ischaemic brain, but this mechanism only partially explained the protective effect of anti-CD49d. In a previous study (Liesz *et al*., 2009*b*), we have shown that T cells are the major source of IFN-γ in the ischaemic brain. Remarkably, depletion of $CD8^+$ cells was as effective as of $CD4^+$ cells in reducing infarct size, suggesting an additional cytotoxic pathway. Indeed, absence of perforin, the key cytotoxic mechanism of CD8+ cells, substantially improved outcome. This is, to our knowledge, the first report regarding perforin-mediated cytotoxicity after brain ischaemia and is consistent with a previous study on the role of granzyme B—a mediator downstream of perforin—in experimental ischaemia (Chaitanya *et al*., 2010). Besides $CD8^+$ T cells, NK cells are also a possible source of perforin (Moretta *et al*., 2008) that invade the ischaemic brain (Gelderblom *et al*., 2009). However, we have analysed the contribution of NK cells in post-ischaemic neuroinflammation by depleting this cell-population with NK1.1-specific antibodies and did not detect a significant influence on the resulting infarct volume in models of permanent or reversible MCAO (data not shown).

Regulatory T cells are an immunosuppressive subpopulation of T cells that are neuroprotective after experimental ischaemic stroke (Liesz *et al*., 2009*b*). The main function of regulatory T cells is to prevent overactivation of the immune system (Maloy and Powrie, 2001; O'Garra and Vieira, 2004; Sakaguchi *et al*., 2007). However, anti-CD49d treatment did not appear to result from enhancement of regulatory T cells in the present study because the number of regulatory T cells and other lymphocyte subpopulations in the brain was diminished equally by the antibody. Instead, endogenous regulatory T cells and anti-CD49d treatment may affect similar deleterious lymphocyte pathways by different means. While regulatory T cells reduce the activation of invading lymphocytes as measured by cellular IFN-γ production (Liesz *et al*., 2009*b*), anti-CD49d treatment prevents the invasion of lymphocytes.

VLA-4 mediated endothelial leukocyte adhesion can take place via different vascular ligands including VCAM-1 and fibronectin

Figure 7 Continued

of micro western blot assays for VCAM-1 expression, normalized for actin loading control, in control animals and anti-CD49d treated animals 6 days after MCAO. Dots represent individual mice and bars indicate mean values. (**E**) Image of a representative brain section stained for rat IgG antibodies 6 days after MCAO of mice treated intraperitoneally with rat anti-mouse VCAM-specific antibodies 24 h prior and 3 days after MCAO induction. (**F**) Infarct volumes 6 days after MCAO in mice receiving intraperitoneal administrations of IgG control antibodies or VCAM-specific antibodies at 24 h before and 3 days after ischaemia induction (n = 10 per group, two individual experiments). (**G**) Representative micro western blot and dot plot analysis for VCAM-1 protein expression at 5 days after MCAO in mice treated with negative control small interfering RNA (siRNA) or VCAM-specific small interfering RNA. (**H**) Infarct volumes at 6 days after MCAO in mice receiving control small interfering RNA intravenously or VCAM-1 specific small interfering RNA or additionally CD49d-specific antibodies intraperitoneally (i.p.). Control groups received IgG isotype control antibody (n = 11 per group, three individual experiments). (**I**) Analysis of granulocyte (*left*) and T cell (*right*) cell counts per one complete section of the ischaemic hemisphere at 6 days after MCAO (n = 5 per group). Filled bars = control small interfering RNA; open bars = VCAM-1 small interfering RNA treatment; Pos = positive control.

(Elices *et al*., 1990; Vajkoczy *et al*., 2001; Engelhardt, 2008). After *in vivo* silencing of VCAM-1, α4-integrin blockade did not achieve any additional cerebroprotection, indicating that VCAM-1 is the main endothelial counterpart of VLA-4 after brain ischaemia. In contrast to the lack of cerebroprotection by VCAM-1-specific antibodies in a previous (Justicia *et al*., 2006) and the present study, *in vivo* hydrodynamic VCAM-1 silencing using small interfering RNA—a technique that to our knowledge has not been applied in cerebral ischaemia previously—effectively reduced the infarct size and attenuated leukocyte infiltration and cerebral IFN-γ levels. RNA interference by hydrodynamic small interfering RNA delivery is a highly efficient method for targeting endothelial protein expression (Hino *et al*., 2006; Lewis and Wolff, 2007) but non-specific immunostimulatory effects by small interfering RNA need to be considered (Robbins *et al*., 2009). Although physical impact on the endothelium has been reported as the basis for this potent RNA delivery strategy, previous studies observed only transient and reversible endothelial changes and normal morphology 30 min after injection (Suda *et al*., 2007). In our study, VCAM-1-targeting proved to be specific, and control animals receiving control small interfering RNAs had no detectable effects compared with naïve animals. Importantly, our experiments reveal cross-signalling between activated leukocytes and their endothelial counterpart VCAM-1 as anti-CD49d treatment attenuated post-ischaemic VCAM-1 induction. This phenomenon might be attributed to the inhibition of leukocyte-endothelial interaction, since VLA-4–VCAM-1 binding is known to induce endothelial activation with consecutive structural changes (Muller, 2009), production of reactive oxygen species, and secretion of cytokines and matrix metalloproteinases (Hordijk, 2006).

Following cerebral ischaemia and other severe brain injury, the systemic immune system undergoes substantial changes that frequently render stroke patients susceptible to infectious complications (Meisel *et al*., 2005; Chamorro *et al*., 2007). To model this setting, ischaemic mice were challenged with *Streptococcus pneumoniae* (Stegemann *et al*., 2009). Importantly, treatment with CD49d-specific antibodies did not exacerbate bacterial infection, suggesting that this immunomodulatory approach is safe from a microbiological perspective.

In conclusion, despite profound differences in the primary pathogenesis of multiple sclerosis and ischaemic stroke, both disorders share key pathways of adaptive immunity that can be successfully targeted by immunotherapy. Although many aspects of the immune pathogenesis after brain ischaemia remain to be elucidated and additional investigations are necessary before translating the findings into the clinical setting, inhibition of cerebral lymphocyte trafficking appears to be a promising new approach for ischaemic stroke.

Acknowledgements

The authors would like to thank T. Giese for critical methodical input and D. Stefan for excellent technical assistance in flow cytometry, M. Zorn for performing differential blood cell countings at the Core Laboratory Facilities of the University of Heidelberg, Claudia Veltkamp for critical revision of the article, A. Tillmanns-Liesz for assistance in behavioural testing and A. Stojanovic (German Cancer Research Center, Heidelberg, Germany) for providing the *Rag2*$^{-/-}$ mice. A.L. designed and performed experiments, analysed data, and wrote the article; W.Z., E.M., H.B., C.S., S.St. and S.Sch. performed experiments and analysed data; S.K. and L.S. performed experiments; A.C. provided critical input on experimental design and article writing; A.H.D. and D.B. designed experiments and analysed data; R.V. initiated and directed the entire study, designed experiments, analysed data and wrote the article.

Funding

Else-Kröner Fresenius Stiftung; German federal and state governments' Excellence initiative (to R.V.); Else-Kröner-Memorial Scholarship (to R.V.).

Supplementary material

Supplementary material is available at *Brain* online.

References

Baron JL, Madri JA, Ruddle NH, Hashim G, Janeway CA Jr. Surface expression of alpha 4 integrin by CD4 T cells is required for their entry into brain parenchyma. J Exp Med 1993; 177: 57–68.

Barone FC, Feuerstein GZ. Inflammatory mediators and stroke: new opportunities for novel therapeutics. J Cereb Blood Flow Metab 1999; 19: 819–34.

Bartholomaus I, Kawakami N, Odoardi F, Schlager C, Miljkovic D, Ellwart JW, et al. Effector T cell interactions with meningeal vascular structures in nascent autoimmune CNS lesions. Nature 2009; 462: 94–8.

Becker K, Kindrick D, Relton J, Harlan J, Winn R. Antibody to the alpha4 integrin decreases infarct size in transient focal cerebral ischaemia in rats. Stroke 2001; 32: 206–11.

Chaitanya GV, Schwaninger M, Alexander JS, Babu PP. Granzyme-b is involved in mediating post-ischaemic neuronal death during focal cerebral ischaemia in rat model. Neuroscience 2010; 165: 1203–16.

Chamorro A, Urra X, Planas AM. Infection after acute ischaemic stroke: a manifestation of brain-induced immunodepression. Stroke 2007; 38: 1097–103.

Cook-Mills JM, Deem TL. Active participation of endothelial cells in inflammation. J Leukoc Biol 2005; 77: 487–95.

Damle NK, Klussman K, Linsley PS, Aruffo A. Differential costimulatory effects of adhesion molecules B7, ICAM-1, LFA-3, and VCAM-1 on resting and antigen-primed CD4+ T lymphocytes. J Immunol 1992; 148: 1985–92.

Davies CA, Loddick SA, Toulmond S, Stroemer RP, Hunt J, Rothwell NJ. The progression and topographic distribution of interleukin-1beta expression after permanent middle cerebral artery occlusion in the rat. J Cereb Blood Flow Metab 1999; 19: 87–98.

del Zoppo GJ, Becker KJ, Hallenbeck JM. Inflammation after stroke: is it harmful? Arch Neurol 2001; 58: 669–72.

Dirnagl U. Inflammation in stroke: the good, the bad, and the unknown. Ernst Schering Res Found Workshop 2004; 87–99.

Dirnagl U. Bench to bedside: the quest for quality in experimental stroke research. J Cereb Blood Flow Metab 2006; 26: 1465–78.

Dirnagl U, Iadecola C, Moskowitz MA. Pathobiology of ischaemic stroke: an integrated view. Trends Neurosci 1999; 22: 391–7.

Donnan GA, Fisher M, Macleod M, Davis SM. Stroke. Lancet 2008; 371: 1612–23.

Ecker RC, Rogojanu R, Streit M, Oesterreicher K, Steiner GE. An improved method for discrimination of cell populations in tissue sections using microscopy-based multicolor tissue cytometry. Cytometry A 2006; 69: 119–23.

Elices MJ, Osborn L, Takada Y, Crouse C, Luhowskyj S, Hemler ME, et al. VCAM-1 on activated endothelium interacts with the leukocyte integrin VLA-4 at a site distinct from the VLA-4/fibronectin binding site. Cell 1990; 60: 577–84.

Emsley HC, Hopkins SJ. Acute ischaemic stroke and infection: recent and emerging concepts. Lancet Neurol 2008; 7: 341–53.

Engelhardt B. Immune cell entry into the central nervous system: involvement of adhesion molecules and chemokines. J Neurol Sci 2008; 274: 23–6.

Engelhardt B, Kappos L. Natalizumab: targeting alpha4-integrins in multiple sclerosis. Neurodegener Dis 2008; 5: 16–22.

Engelhardt B, Laschinger M, Schulz M, Samulowitz U, Vestweber D, Hoch G. The development of experimental autoimmune encephalomyelitis in the mouse requires alpha4-integrin but not alpha4beta7-integrin. J Clin Invest 1998; 102: 2096–105.

Engelhardt B, Sorokin L. The blood-brain and the blood-cerebrospinal fluid barriers: function and dysfunction. Semin Immunopathol 2009; 31: 497–511.

Frangogiannis NG, Smith CW, Entman ML. The inflammatory response in myocardial infarction. Cardiovasc Res 2002; 53: 31–47.

Gee JM, Kalil A, Shea C, Becker KJ. Lymphocytes: potential mediators of postischaemic injury and neuroprotection. Stroke 2007; 38: 783–8.

Gelderblom M, Leypoldt F, Steinbach K, Behrens D, Choe CU, Siler DA, et al. Temporal and spatial dynamics of cerebral immune cell accumulation in stroke. Stroke 2009; 40: 1849–57.

Harris AK, Ergul A, Kozak A, Machado LS, Johnson MH, Fagan SC. Effect of neutrophil depletion on gelatinase expression, edema formation and hemorrhagic transformation after focal ischaemic stroke. BMC Neurosci 2005; 6: 49.

Herweijer H, Wolff JA. Gene therapy progress and prospects: hydrodynamic gene delivery. Gene Ther 2007; 14: 99–107.

Hino T, Yokota T, Ito S, Nishina K, Kang YS, Mori S, et al. In vivo delivery of small interfering RNA targeting brain capillary endothelial cells. Biochem Biophys Res Commun 2006; 340: 263–7.

Hordijk PL. Endothelial signalling events during leukocyte transmigration. FEBS J 2006; 273: 4408–15.

Hurn PD, Subramanian S, Parker SM, Afentoulis ME, Kaler LJ, Vandenbark AA, et al. T- and B-cell-deficient mice with experimental stroke have reduced lesion size and inflammation. J Cereb Blood Flow Metab 2007; 27: 1798–805.

Ibbotson GC, Doig C, Kaur J, Gill V, Ostrovsky L, Fairhead T, et al. Functional alpha4-integrin: a newly identified pathway of neutrophil recruitment in critically ill septic patients. Nat Med 2001; 7: 465–70.

Jander S, Kraemer M, Schroeter M, Witte OW, Stoll G. Lymphocytic infiltration and expression of intercellular adhesion molecule-1 in photochemically induced ischaemia of the rat cortex. J Cereb Blood Flow Metab 1995; 15: 42–51.

Jander S, Pohl J, Gillen C, Schroeter M, Stoll G. Vascular cell adhesion molecule-1 mRNA is expressed in immune-mediated and ischaemic injury of the rat nervous system. J Neuroimmunol 1996; 70: 75–80.

Justicia C, Martin A, Rojas S, Gironella M, Cervera A, Panes J, et al. Anti-VCAM-1 antibodies did not protect against ischaemic damage either in rats or in mice. J Cereb Blood Flow Metab 2006; 26: 421–32.

Kleinschnitz C, Schwab N, Kraft P, Hagedorn I, Dreykluft A, Schwarz T, et al. Early detrimental T cell effects in experimental cerebral ischaemia are neither related to adaptive immunity nor thrombus formation. Blood 2010; 115: 3835–42.

Lambertsen KL, Meldgaard M, Ladeby R, Finsen B. A quantitative study of microglial-macrophage synthesis of tumor necrosis factor during acute and late focal cerebral ischaemia in mice. J Cereb Blood Flow Metab 2005; 25: 119–35.

Laschinger M, Engelhardt B. Interaction of alpha4-integrin with VCAM-1 is involved in adhesion of encephalitogenic T cell blasts to brain endothelium but not in their transendothelial migration in vitro. J Neuroimmunol 2000; 102: 32–43.

Lewis DL, Wolff JA. Systemic siRNA delivery via hydrodynamic intravascular injection. Adv Drug Deliv Rev 2007; 59: 115–23.

Liesz A, Hagmann S, Zschoche C, Adamek J, Zhou W, Sun L, et al. The spectrum of systemic immune alterations after murine focal ischaemia: immunodepression versus immunomodulation. Stroke 2009a; 40: 2849–58.

Liesz A, Suri-Payer E, Veltkamp C, Doerr H, Sommer C, Rivest S, et al. Regulatory T cells are key cerebroprotective immunomodulators in acute experimental stroke. Nat Med 2009b; 15: 192–9.

Lo EH. T time in the brain. Nat Med 2009; 15: 844–6.

Lo EH, Dalkara T, Moskowitz MA. Mechanisms, challenges and opportunities in stroke. Nat Rev Neurosci 2003; 4: 399–415.

Maloy KJ, Powrie F. Regulatory T cells in the control of immune pathology. Nat Immunol 2001; 2: 816–22.

Matsuo Y, Onodera H, Shiga Y, Nakamura M, Ninomiya M, Kihara T, et al. Correlation between myeloperoxidase-quantified neutrophil accumulation and ischaemic brain injury in the rat. Effects of neutrophil depletion. Stroke 1994; 25: 1469–75.

Meisel C, Schwab JM, Prass K, Meisel A, Dirnagl U. Central nervous system injury-induced immune deficiency syndrome. Nat Rev Neurosci 2005; 6: 775–86.

Moretta A, Marcenaro E, Parolini S, Ferlazzo G, Moretta L. NK cells at the interface between innate and adaptive immunity. Cell Death Differ 2008; 15: 226–33.

Muller WA. Mechanisms of transendothelial migration of leukocytes. Circ Res 2009; 105: 223–30.

O'Garra A, Vieira P. Regulatory T cells and mechanisms of immune system control. Nat Med 2004; 10: 801–5.

Polman CH, O'Connor PW, Havrdova E, Hutchinson M, Kappos L, Miller DH, et al. A randomized, placebo-controlled trial of natalizumab for relapsing multiple sclerosis. N Engl J Med 2006; 354: 899–910.

Relton JK, Sloan KE, Frew EM, Whalley ET, Adams SP, Lobb RR. Inhibition of alpha4 integrin protects against transient focal cerebral ischaemia in normotensive and hypertensive rats. Stroke 2001; 32: 199–205.

Rice GP, Hartung HP, Calabresi PA. Anti-alpha4 integrin therapy for multiple sclerosis: mechanisms and rationale. Neurology 2005; 64: 1336–42.

Robbins M, Judge A, MacLachlan I. siRNA and innate immunity. Oligonucleotides 2009; 19: 89–102.

Rose DM, Han J, Ginsberg MH. Alpha4 integrins and the immune response. Immunol Rev 2002; 186: 118–24.

Russell JH, Ley TJ. Lymphocyte-mediated cytotoxicity. Ann Rev Immunol 2002; 20: 323–70.

Sakaguchi S, Wing K, Miyara M. Regulatory T cells - a brief history and perspective. Eur J Immunol 2007; 37 (Suppl. 1): S116–23.

Schroder K, Hertzog PJ, Ravasi T, Hume DA. Interferon-gamma: an overview of signals, mechanisms and functions. J Leukocyte Biol 2004; 75: 163–89.

Schurer L, Grogaard B, Gerdin B, Kempski O, Arfors KE. Leucocyte depletion does not affect post-ischaemic nerve cell damage in the rat. Acta Neurochir 1991; 111: 54–60.

Shichita T, Sugiyama Y, Ooboshi H, Sugimori H, Nakagawa R, Takada I, et al. Pivotal role of cerebral interleukin-17-producing gammadeltaT cells in the delayed phase of ischaemic brain injury. Nat Med 2009; 15: 946–50.

Stegemann S, Dahlberg S, Kroger A, Gereke M, Bruder D, Henriques-Normark B, et al. Increased susceptibility for superinfection with Streptococcus pneumoniae during influenza virus infection is not caused by TLR7-mediated lymphopenia. PLoS One 2009; 4: e4840.

Steinman L. Blocking adhesion molecules as therapy for multiple sclerosis: natalizumab. Nat Rev Drug Discov 2005; 4: 510–8.

Suda T, Gao X, Stolz DB, Liu D. Structural impact of hydrodynamic injection on mouse liver. Gene Ther 2007; 14: 129–37.

Swanson RA, Morton MT, Tsao-Wu G, Savalos RA, Davidson C, Sharp FR. A semiautomated method for measuring brain infarct volume. J Cereb Blood Flow Metab 1990; 10: 290–3.

Takagi J, Springer TA. Integrin activation and structural rearrangement. Immunol Rev 2002; 186: 141–63.

Trapani JA, Smyth MJ. Functional significance of the perforin/granzyme cell death pathway. Nat Rev Immunol 2002; 2: 735–47.

Vajkoczy P, Laschinger M, Engelhardt B. Alpha4-integrin-VCAM-1 binding mediates G protein-independent capture of encephalitogenic T cell blasts to CNS white matter microvessels. J Clin Invest 2001; 108: 557–65.

van Seventer GA, Newman W, Shimizu Y, Nutman TB, Tanaka Y, Horgan KJ, et al. Analysis of T cell stimulation by superantigen plus major histocompatibility complex class II molecules or by CD3 monoclonal antibody: costimulation by purified adhesion ligands VCAM-1, ICAM-1, but not ELAM-1. J Exp Med 1991; 174: 901–13.

Wang Q, Tang XN, Yenari MA. The inflammatory response in stroke. J Neuroimmunol 2006; 184 (1-2): 53–68.

Yednock TA, Cannon C, Fritz LC, Sanchez-Madrid F, Steinman L, Karin N. Prevention of experimental autoimmune encephalomyelitis by antibodies against alpha 4 beta 1 integrin. Nature 1992; 356: 63–6.

Yilmaz G, Arumugam TV, Stokes KY, Granger DN. Role of T lymphocytes and interferon-gamma in ischaemic stroke. Circulation 2006; 113: 2105–12.

Zhang L, Schallert T, Zhang ZG, Jiang Q, Arniego P, Li Q, et al. A test for detecting long-term sensorimotor dysfunction in the mouse after focal cerebral ischaemia. J Neurosci Methods 2002; 117: 207–14.

Zipp F, Aktas O. The brain as a target of inflammation: common pathways link inflammatory and neurodegenerative diseases. Trends Neurosci 2006; 29: 518–27.

Zwacka RM, Zhang Y, Halldorson J, Schlossberg H, Dudus L, Engelhardt JF. CD4(+) T-lymphocytes mediate ischaemia/reperfusion-induced inflammatory responses in mouse liver. J Clin Invest 1997; 100: 279–89.